

## Original Article

# Bioinformatics evaluation of a novel angiogenesis related genes-based signature for predicting prognosis and therapeutic efficacy in patients with gastric cancer

Ning Ma<sup>1\*</sup>, Jie Li<sup>2\*</sup>, Ling Lv<sup>3\*</sup>, Chunhua Li<sup>4</sup>, Kainan Li<sup>5</sup>, Bin Wang<sup>2</sup>

<sup>1</sup>Department of Clinical Laboratory, 905th Hospital of PLA, Naval Medical University, 1328 Huashan Road, Shanghai 200050, P. R. China; <sup>2</sup>Department of Oncology, Changhai Hospital, Naval Medical University, 168 Changhai Road, Shanghai 200433, P. R. China; <sup>3</sup>Disaster Preparedness and First Aid Training Center of RCSC Shangdong Branch, Aoti Middle Road #5316, Jinan 250101, Shandong, P. R. China; <sup>4</sup>Department of Oncology, The Second Affiliated Hospital of Shandong University of Traditional Chinese Medicine, Jingba Road #1, Jinan 250001, Shandong, P. R. China; <sup>5</sup>Department of Oncology, Shandong Provincial Third Hospital, Cheeloo College of Medicine, Shandong University, 11 Wuyingshan Middle Road, Jinan 250031, Shandong, P. R. China. \*Equal contributors.

Received March 17, 2022; Accepted May 23, 2022; Epub July 15, 2022; Published July 30, 2022

**Abstract:** Objective: Tumor angiogenesis plays a pivotal role in the development and metastasis of tumors. This study aimed to elucidate the association between angiogenesis-related genes (ARGs) and the prognosis of patients with gastric cancer (GC). Methods: Transcriptomics and clinical data of GC samples were obtained from The Cancer Genome Atlas (TCGA) as the training group and those from Gene Expression Omnibus (GEO, including GSE26253, GSE26091 and GSE66229) as the validation groups. Single-sample gene set enrichment analysis (ssGSEA) was performed for gene set enrichment analysis on the gene set of angiogenesis and divided patients into high- or low-ARG group. Subsequently, to improve the availability of the ARG signature, a ARGs subtype predictor was then constructed by integrating of four machine learning methods, including support vector machine (SVM), least absolute shrinkage and selection operator (LASSO) regression, Random Forest and Boruta (RFB) and extreme gradient boosting (XGBoost). Kaplan-Meier and receiver operating characteristic curves were used to evaluate the performance of prognosis prediction. The EPIC and xCELL method were used to calculate the profile of tumor-infiltrated immune cells. Results: The expression levels of a total of 36 ARGs that correlated with the survival of patients with GC were identified and utilized to establish an ARG-related prognosis signature. The area under the curve for predicting overall survival (OS) in the training group at the 1-, 3- and 5-year was 0.61, 0.64 and 0.76, respectively, and this was further validated using three independent GEO datasets. Moreover, the ARG signatures were significantly correlated with cancer-associated fibroblasts (CAFs), and GC patients that exhibited both high ARG expression level and matrix CAFs level had the most inferior outcomes. The multiple machine learning algorithms were applied to establish a 10-gene ARG subtype predictor, and notably, a high ARG-subtype predictor score was associated with reduced efficacy of immunotherapy, and potential anti-HER2 or FGFR4 therapy, but an increased sensitivity to anti-angiogenesis-related therapy. Conclusion: The novel ARGs-based classification may act as a potential prognostic predictor for GC and be used as a guidance for clinicians in selecting potential responders for immunotherapy and targeted therapy.

**Keywords:** Angiogenesis, gastric cancer, TCGA, cancer-associated fibroblasts, immune cell infiltration, immunotherapy

## Introduction

Gastric cancer (GC) is the fifth most common malignancy and the third most common cause of cancer-related death worldwide [1]. Despite of ongoing advances in treatment strategies, patient outcomes remain poor [2]. GC is a high-

ly heterogeneous disease with differing features, including locations, histological types, molecular classifications and biological behaviors [3]. However, primary tumors with biological heterogeneity are often missed by conventional diagnostic methods, which are often based on TNM staging [4]. Therefore, a novel

risk model for the identification of patients with a high risk of developing GC is required to provide a guideline for personalized medicine in patients with GC.

Angiogenesis is defined as the process in which new capillaries grow from pre-existing vessels, and has been characterized as a vital factor for the proliferation, growth and metastasis of tumor cells in multiple solid tumors [5]. It is considered as one of the hallmarks of cancer, attributing to cancer cell growth by providing oxygen and nutrients, delivering molecules that confer immune and treatment resistance, and facilitating metastasis [6]. Results of previous studies have revealed that a wide variety of genes play crucial roles in angiogenesis, such as vascular endothelial growth factors (VEGFs) and their receptors (VEGFRs), which have been previously established in angiogenic signaling pathways [7]. Results of a previous study revealed that active angiogenesis may result in therapeutic failure and poor outcomes in patients with GC [8]. Meanwhile, Feng et al. demonstrated that angiogenesis signaling was significantly associated with the cytotoxic function in patients with GC with a highly infiltrated immune niche [9]. However, the clinical relevance of angiogenesis-related genes (ARGs) in GC is yet to be fully elucidated.

Cancer-associated fibroblasts (CAFs) are the predominant component of the tumor microenvironment (TME), and are involved in critical processes within the TME, including extracellular matrix (ECM) remodeling, reciprocal signaling interactions with cancer cells and crosstalk with infiltrating inflammatory cells [10]. Accumulating evidence indicates that CAFs play crucial roles in the growth, invasion and progression of tumors, and are associated with a poor prognosis in various solid tumors [11-13]. In addition, previous studies have revealed that angiogenesis played a pivotal role in the CAF promotion of invasion and metastasis of tumors [14]. However, the interaction between CAF and angiogenesis, and the outcomes of patients with GC have not been fully elucidated.

Thus, in this study, we sought to evaluate the comprehensive role of ARGs in the prognosis of GC and then develop a robust signature to predict GC patients' survival based on the ARG related feature using the transcriptomics data from The Cancer Genome Atlas (TCGA) and

Gene Expression Omnibus (GEO). Special interests were given to analyze correlation between the ARG signatures and TME in GC. Subsequently, an ARG subtype predictor was established to distinguish the two subtypes in patients with GC, giving stratification not only in survival but also in systemic treatments including immunotherapy.

### Methods and materials

#### *Acquisition of gastric cancer datasets and selection of angiogenesis-related genes*

The RNA-seq (RNA-sequencing) datasets and clinical features of the TCGA-GC cohort from the TCGA database (<http://xena.ucsc.edu/>) were downloaded as the training group. The following criteria were applied for validation datasets selection in the Gene Expression Omnibus (GEO, <https://www.ncbi.nlm.nih.gov/geo/>) database: (i) tumor tissue samples were from gastric cancer; (ii) the dataset must have a complete record of the overall survival data; (iii) the expression data must be generated using a genome-wide gene expression method; (iv) the sample size for analysis should be over than 100. Then, GSE26253 (containing 432 GC samples), GSE26901 (109 GC samples) and GSE66229 (185 GC samples) were obtained from the GEO as the validation groups.

The Angiogenesis-related genes, a total of 36 genes, were downloaded from Molecular Signatures Database (<http://www.gsea-msigdb.org/gsea/msigdb/>, MSigDB-Hallmark version 7.4), as the ARGs gene set.

#### *The construction of the ARGs signature based on single-sample gene set enrichment analysis (ssGSEA)*

The enrichment score and the absolute enrichment degree of a gene set in each sample were calculated using ssGSEA by an empirical cumulative distribution function according to the given ARGs expression profile. The Gene Set Variation Analysis (GSVA) package was used to calculate the ARGs ssGSEA score of 414 samples from TCGA-STAD. The limma package in R was applied to assess the scores in different tissue types and survival statuses. GSEA (version 4.1.0.24) was performed for gene set enrichment analysis (GSEA) on the gene set (angiogenesis related genes) with 1000 permu-

## Angiogenesis related genes-associated signature of gastric cancer

tations using gene expression profiles of 414 tumor samples. The patients were divided into high and low ARG score (ssGSEA score) groups for further analysis.

### *Tumor-infiltrated immune cell analysis*

We firstly evaluated correlation of CYT, ESTIMATE, HLA, ICG, TIL, tumor purity and ARG score by Spearman's analysis. The EPIC and xCELL methods were used to calculate the infiltration abundance of immune cells in both TCGA and GEO datasets according to the "EPIC and xCELL" package including eight immune cells in EPIC package (version 1.1.5) and thirty-six immune cells in the XCELL package (<https://xcell.ucsf.edu/>), respectively.

### *Construction and validation of the ARGs subtype predictor by multiple machine learning methods*

The 414 GC patients were classified into training (N=331) and testing (N=83) sets based on a ratio of 4:1. First, in the training set, the most important group-relevant features were selected using support vector machine (SVM), least absolute shrinkage and selection operator (LASSO) regression, Random Forest and Boruta (RFB), and extreme gradient boosting (XGBoost) analyses by calculating the importance score for each variable via the glmnet, rms, e1071, caret, randomForest, Boruta, and XGBoost packages in R [15-17]. The expression of the ARGs-related differentially expressed genes (DEGs) were identified using a fold change cutoff value of 2 and a false discovery rate (FDR) <0.05. Then the identified DEGs were selected as the input variable (independent variables), and the status of subtypes was selected as the outcome (binary dependent variables, 0 or 1). The receiver operating characteristic (ROC) curves were used to evaluate the performance of the four machine learning algorithms for feature selection in the training set, and the areas under the ROC curve (AUCs) were subsequently compared. Afterwards, the most critical subtype-related genes were obtained from the intersecting genes among the LASSO, SVM, RFB and XGBoost analyses, and were visualized using a Venn diagram. Finally, the critical genes were analyzed by multivariate logistic regression analysis and used to construct the predictive model, which was termed by 'Subtype Predictor'. The ROC curve

was used to investigate the performance of the subtype predictor which was further used to determine the optimal cutoff values in discriminating different subtypes, as well as the AUC, sensitivity, specificity and accuracy. Finally, the test set was used to validate the predictive performance of the subtype predictor in a similar way.

### *The evaluation of the efficacy anti-angiogenesis therapy response*

The data from the Genomics of Drug Sensitivity in Cancer (GDSC, <https://www.cancerrxgene.org/>) were downloaded to explore the response of anti-angiogenesis therapy regimes between high- and low-risk groups. The index of half-maximal inhibitory concentration ( $IC_{50}$ ) was used for the response evaluation.

### *Statistical analysis*

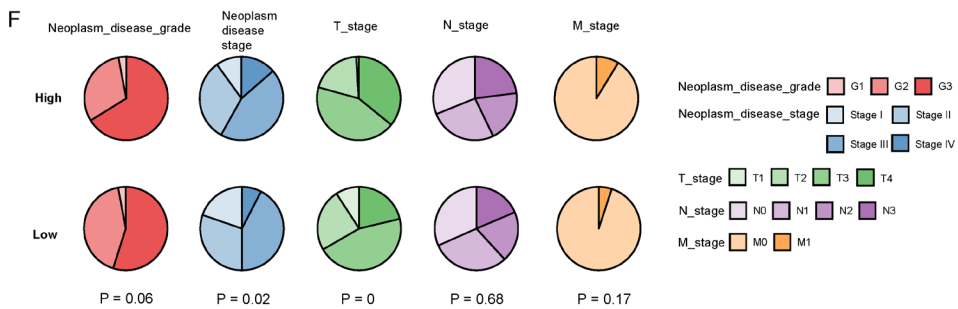
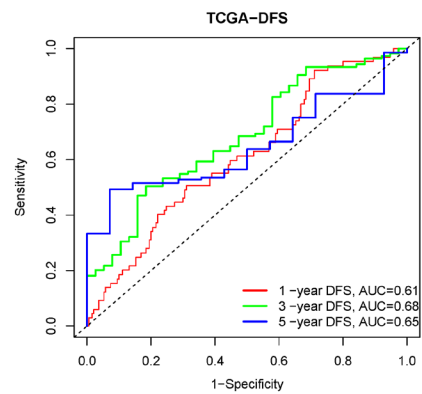
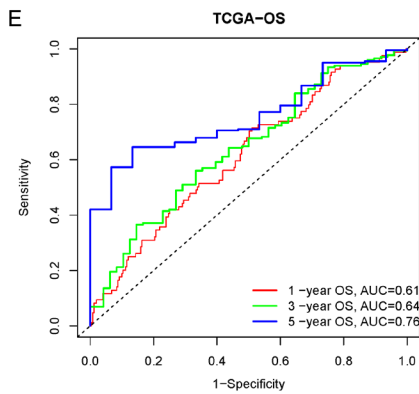
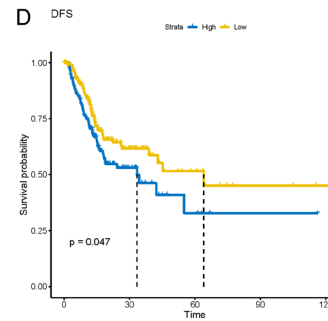
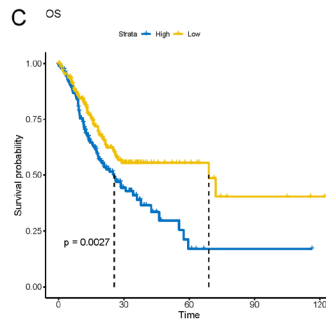
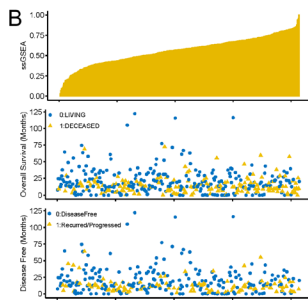
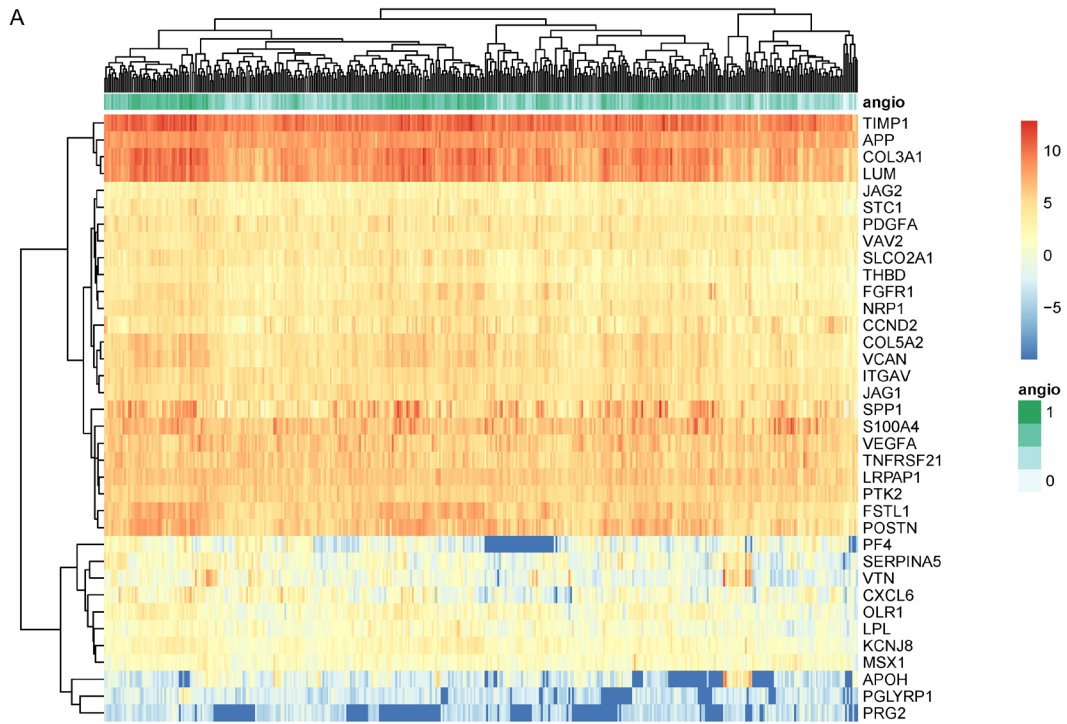
R software (version 3.6.0) was utilized to implement the all-statistical analyses and plots. The  $X^2$  test was executed to assess the correlation between risk score and clinical characteristics. The significant difference of OS between the low ARGs risk score group and high ARGs risk score group was analyzed by Kaplan-Meier curve and the log-rank test. The relationship between risk scores and OS was evaluated by using the univariate and multivariate Cox proportional hazard regression analyses. The sensitivity and specificity of gene signature risk score in predicting survival were detected using ROC analysis. The prognostic accuracy was estimated by the area under ROC curve (AUC) analysis. In all analyses,  $P$ -value <0.05 was set to be statistically significant.

## Results

### *The identification and prognostic analysis of candidate ARGs in the cohort from TCGA*

To investigate ARG variation in GC, a total of 36 ARGs with expression profiles in the cohort obtained from TCGA were selected (**Figure 1A**). Based on the median value of ARG score (ssGSEA scores), all patients with GC included in this cohort were stratified into high-ARG and low-ARG groups (**Figure 1B**, the top panel). The middle panel and bottom panel displayed in **Figure 1B** revealed that the survival rates, including both the OS and DFS rates of patients in the high-risk group differed from those in the

# Angiogenesis related genes-associated signature of gastric cancer



## Angiogenesis related genes-associated signature of gastric cancer

**Figure 1.** The identification and prognostic analysis of the candidate angiogenesis-related genes in the TCGA cohort. A: The heatmap of the 36 angiogenesis-related genes' expression in gastric cancer tissues. B: The distribution and median value of the ssGSEA scores in the TCGA cohort (up panel). The distribution of OS, OS status, and risk score in the TCGA cohort (middle panel). The distribution of DFS, DFS status, and risk score in the TCGA cohort. C: The Kaplan-Meier curves for the OS of patients in the TCGA cohort, which was divided into high- and low-ARG group. D: The Kaplan-Meier curves for the DFS of patients in the TCGA cohort, which was divided into high-risk group and low-risk group. E: ROC (Receiver operating characteristic) curves showing the 1-, 3-, and 5-year OS and DFS predictive efficiency of the ARGs-signature in the TCGA cohorts. F: The analyses of clinical features between high- and low-ARGs prognosis score groups in GC cohort. ARG: angiogenesis-related genes; OS: overall survival; DFS: disease-free survival; ROC: receiver operating characteristic.

low-risk group. Moreover, compared with those in the low-ARG group, the OS and DFS of patients in the high-risk group were significantly shorter (**Figure 1C** and **1D**). The AUC value predicted that the 1-, 3- and 5-year OS in the training cohort was 0.61, 0.64 and 0.76, respectively, and the AUC value predicted that the 1-, 3- and 5-year DFS was 0.61, 0.68 and 0.65, respectively (**Figure 1E**). Subsequently, the clinical features of patients with high- or low-ARG prognosis scores were investigated. A high-ARG score was significantly correlated with tumor stage (T) and neoplasm disease stage, as more patients with T4 and/or stage IV disease were presented in the high-ARG group (**Figure 1F**). We also compared the expression level 36 ARGs between normal and tumor samples in TCGA-GC and other 4 GEO datasets (including GSE13195, GSE13911, GSE27342, GSE63089), and found that the majority of the ARGs were overexpressed in the tumor samples, except SERPINA5 and PGLYRP1 (**Figure S1**).

### *ARG signatures independently predict OS and DFS*

In order to validate whether the newly-constructed ARG signature could be utilized to predict the prognosis of patients with GC as an independent risk factor, various clinicopathological parameters were tested between high-risk and low-risk score groups. In the TCGA cohort, the univariate analysis revealed that ARGs ( $P=0.002$ ), T-stage ( $P=0.001$ ), N-stage ( $P<0.001$ ), M-stage ( $P=0.004$ ), neoplasm-disease-stage ( $P<0.001$ ) and neoplasm-disease-grade ( $P=0.021$ ) were markedly correlated with OS. Multivariate Cox regression analysis demonstrated that ARGs, M-stage, and neoplasm-disease-grade were independent risk factors of OS. In addition, univariate and multivariate analyses indicated that ARGs as independent risk factors were correlated with a reduced DFS (**Figure 2A**).

Subsequently, patients in the training group were stratified into different subgroups according to clinical characteristics, and the correlation between ssGSEA score and OS of patients with GC was further analyzed. The results of the present study demonstrated that following the stratification of different clinical characteristics, the ARG signature score exhibited an effective prognostic effect in patients with high stage (stage III-IV), tumor stage (T3-4) and N stage (N1-3) GC (**Figure 2B**).

### *Tumor microenvironment profiles related to ARG score*

To further examine the correlation between the ARG score and immune status, ssGSEA was used to calculate the enrichment of different immune cell contents. As demonstrated in **Figure 3A**, a positive correlation between cytolytic activity (CYT) score, ESTIMATE, human leukocyte antigens (HLA), immune checkpoint gene (ICG), tumor-infiltrated lymphocyte (TIL) and ARG score was identified by Spearman's rank analysis. Further investigations demonstrated a significant negative correlation between tumor purity and ARG score (**Figure 3B**). Moreover, EPIC analysis of the tumor-infiltrated lymphocyte profiles demonstrated a statistically significant difference between the high- and low-ARG score groups, including CAFs, T cell CD4+, T cell CD8+, macrophages, endothelial cells and NK cells (**Figure 3C**). The significant difference in CAF content between high- and low-ARG score groups was also determined using XCELL (**Figure 3D**).

### *Association between CAF subtype and ARG signature in patients with GC*

CAFs are one of the most abundant cell types within the cancer stroma, and these were analyzed in patients with GC with different ARG signature scores. According to the results displayed in **Figure 4A-H**, only the matrix CAF

# Angiogenesis related genes-associated signature of gastric cancer

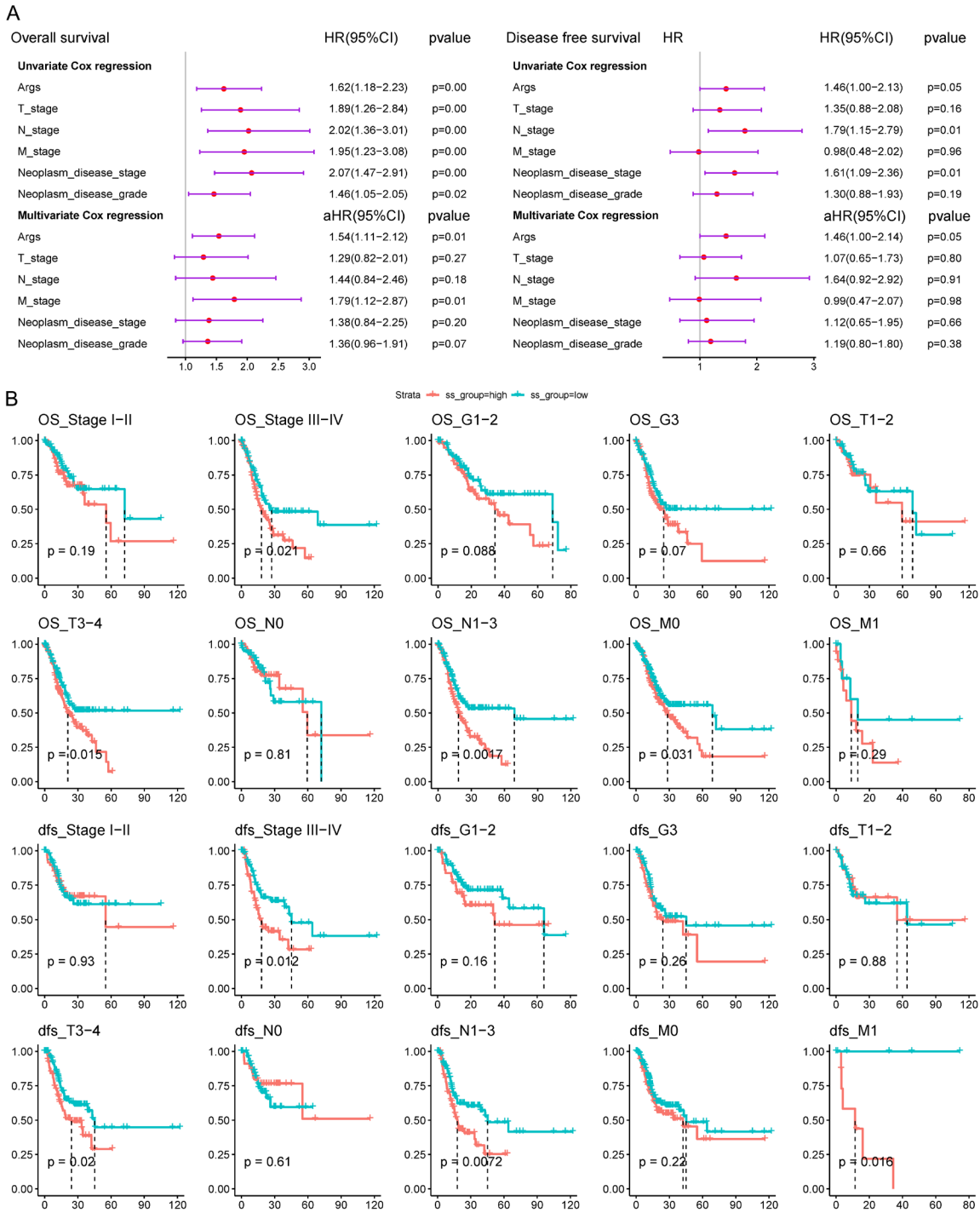


**Figure 2.** The correlation analysis between ARG score and survival in gastric cancer patients. A: Independent prognostic factors for overall survival (OS) and disease-free survival (DFS) in gastric cancer patients. Univariate and multivariate Cox regression analysis was used to identify the relationship between clinicopathological features (including the risk score) and OS and DFS of patients in the training group. B: Stratified analysis of the correlation between ARG score and survival rate (OS and DFS) of patients with gastric cancer in the training group based on different clinical feature, including neoplasm disease stage (Stage I-II and stage II-III), neoplasm disease grade (G1-2 and G3), tumor stage (T1-2 and T3-4), lymph node metastasis stage (N0 and N1-3), long distant metastasis (M0 and M1).

(mCAF) subtype was significantly correlated with reduced OS and DFS, while the remaining

subtypes, including vascular CAF (vCAF) and developmental CAF (dCAF) had no notable



# Angiogenesis related genes-associated signature of gastric cancer

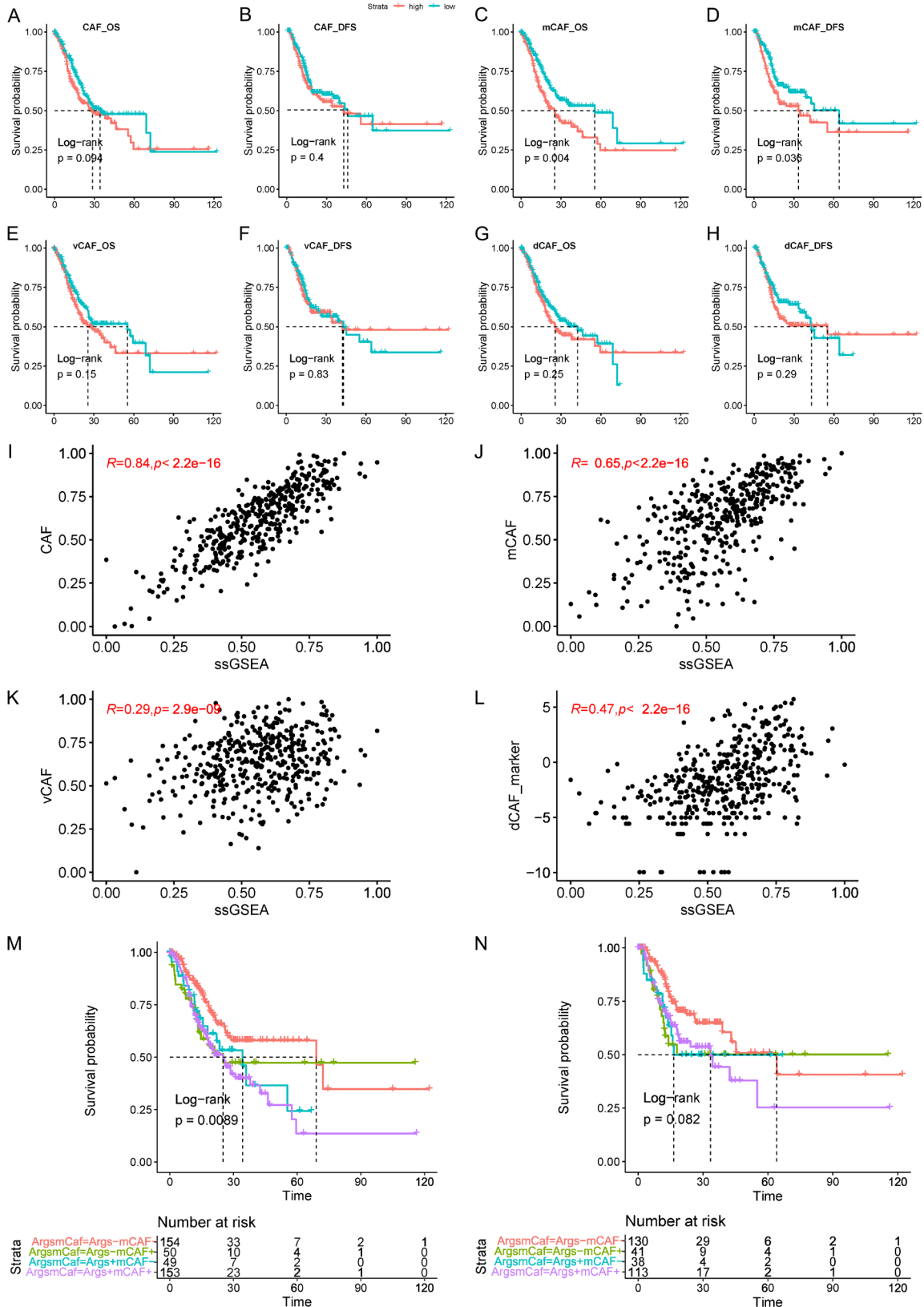


**Figure 4.** Survival analysis of different ARGs and CAFs subgroups. The Kaplan-Meier curves was used for analyzing the OS and DFS of patients in the TCGA cohort, which was divided into high and low CAF density groups (A, B), mCAF (C, D), vCAF (E, F), dCAF (G, H). Spearman's rank order correlation between ARGs and CAFs including total CAF (I,

## Angiogenesis related genes-associated signature of gastric cancer

R=0.84, P=2.2e-16), mCAF (J, R=0.64, P=8e-14), vCAF (K, R=0.31, P=0.00089), dCAF (L, R=0.52, P=5.4e-09). Kaplan-Meier curve of the OS (M) and DFS (N) according to the ARGs signature score and mCAFs contents. CAF: cancer-associated fibroblasts; vascular CAF: vCAF; mCAF: matrix CAF; dCAF: developmental CAF.

mined using Spearman's rank analysis, and results demonstrated that ARGs were positively correlated with various CAFs, including mCAF, vCAF and dCAFs (**Figures 4I-L, S2D**). Moreover, patients with low-ARG score and mCAF content (ARGs-mCAFs-) exhibited the greatest OS rates. By contrast, patients in the high-ARG score and mCAF content group exhibited the poorest prognosis (ARGs+mCAFs+, **Figure 4M, 4N**).

### *Validation of the prognostic ARG signature using external datasets*

To further evaluate the robustness and stability of the identified ARG signatures from the training data set, survival and TME analyses were carried out using GSE26253, GSE26091 and GSE66229 datasets. The same formula was used to calculate ARG scores for patients from the validation cohorts, who were divided into low- and high-subgroups according to the median value of ARG score in each cohort. As demonstrated in the validation results, patients with GC in the low-ARG score subgroup exhibited a significantly superior OS and DFS, compared with patients with high-ARG score in all three validation cohorts (GSE26253: OS, P=0.012; GSE26901: OS, P=0.0012 and DFS, P=0.0026; GSE66229: OS, P=0.00011 and DFS, P=0.003; **Figure 5**). Moreover, the stromal, immune and ESTIMATE scores were markedly increased in the high-ARG score group from the GSE26253 dataset (P<0.001, **Figure S3A**). The correlation between ssGSEA score, TILs and ICGs (CTLA4, TIM3, LAG3 and IDO1) was analyzed using Spearman's rank analysis (**Figure S3B**). A significant correlation was only identified between TIM3 and ARG signature score (R=0.31, P<0.001). Similar results were observed in both GSE26901 and GSE66229 cohorts (**Figures S4 and S5**).

### *Cluster analysis based on ARG expression profiles*

The consensus clustering analysis was performed to further assess the prognostic implication of ARGs in patients with GC from the training cohort (TCGA). The 414 patients with GC from the training group were clustered into

two subgroups, named cluster 1 and 2. The distinction of gene expression levels between cluster 1 and cluster 2 was further validated using principal component analysis (PCA) (**Figure 6A**). Moreover, to investigate the overlap among the classification methods of cluster analysis and ARG score, a Venn diagram was used to demonstrate these results (**Figure 6B**). Results of the survival analysis demonstrated that the OS of patients from cluster 2 was significantly longer, compared with that of patients from cluster 1 (**Figure 6C and 6D**). In addition, stromal, immune and ESTIMATE scores, as well as TIM level were significantly lower in cluster 2 than those in cluster 1 (**Figure 6E, 6F**). Cluster 1 exhibited a significantly increased B cell, CAF, CD4 T cell, endothelial cell, macrophage and uncharacterized cell contents (**Figure 6G**), which was further validated using the XCELL analysis (**Figure 6H**).

### *Establishment and validation of the ARG-related prognostic predictor*

Within the training set, the most critical subtype-relevant features were identified using four machine learning algorithms, according to the expression levels of DEGs. LASSO, RF, SVM and XGBoost analyses were carried out to identify 33, 114, 80 and 110 genes, respectively. A total of 10 critical genes were identified using the Venn diagram, and the genes were shared by the four featured selection algorithms (**Figure 6I**). Subsequently, the diagnostic predictive model was constructed using a multivariate lasso-based logistic regression analysis. ARG subtype predictor was calculated using the formula as follows: risk score = 5.869 + 0.852\* (expression level of DCLK1) + 0.295\* (expression level of PTGIS) + 0.340\* (expression level of NUDT10) + 0.598\* (expression level of ZFH4) + 0.290\* (expression level of PCDH9) + 0.211\* (expression level of CHRDL1) + 0.073\* (expression level of NLGN1) + 0.298\* (expression level of AGTR1) + 0.221\* (expression level of CNTN1) + 0.261\* (expression level of ECRG4). ROC analysis demonstrated an AUC of 0.994 for separating subtypes I and II in the training set (**Figure 6J**). In addition, the subtype predictor also exhibited a high level

## Angiogenesis related genes-associated signature of gastric cancer

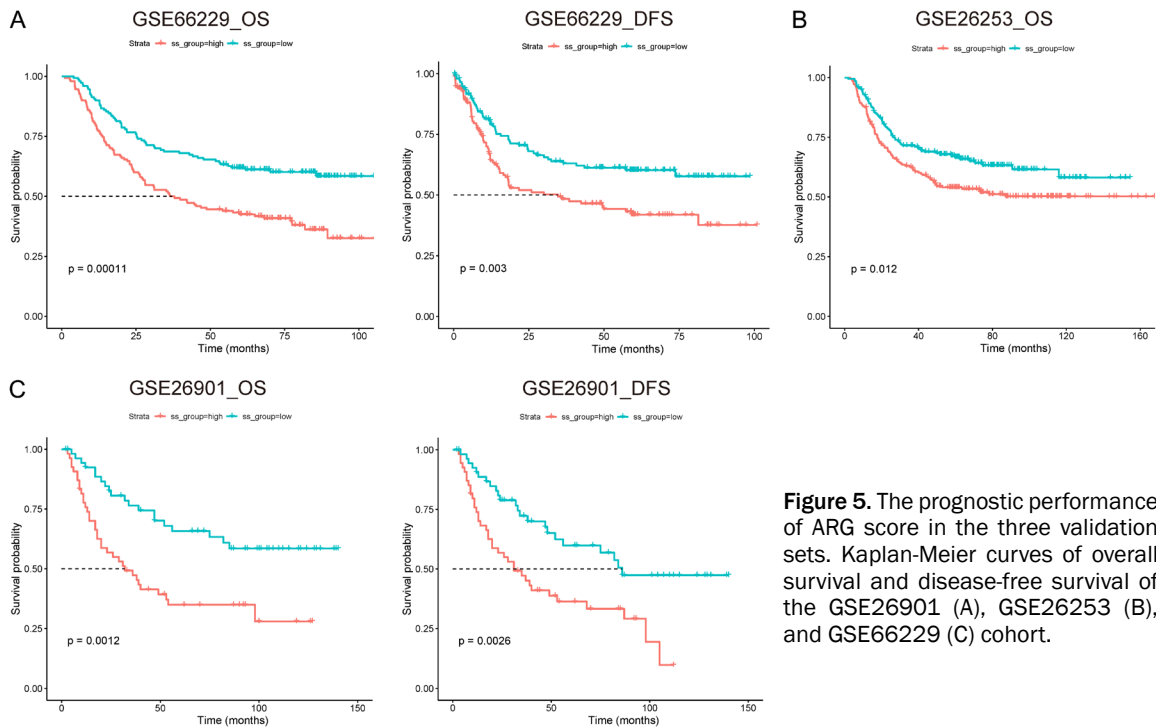


**Figure 5.** The prognostic performance of ARG score in the three validation sets. Kaplan-Meier curves of overall survival and disease-free survival of the GSE26901 (A), GSE26253 (B), and GSE66229 (C) cohort.

of performance in distinguishing the subtypes as evaluated in the test set, with an AUC value of 0.979 (**Figure 6K**). Kaplan-Meier survival analysis revealed that GC patients with a high-risk score presented with significantly inferior OS and PFS in the GSE26901 cohort (**Figure 6L, 6M**). The AUC of predicting 1-, 3- and 5-year OS in the GSE26901 cohort were 0.7, 0.65 and 0.64, respectively, and the AUC of predicting 1-, 3- and 5-year OS in the GSE26901 cohort were 0.66, 0.62 and 0.59, respectively (**Figure 6N, 6O**). The association between risk-score and patient survival was also identified in the GSE66229 cohort, as patients with a high risk score exhibited a significantly reduced DFS and OS (**Figure 6O, 6P**). The prediction efficacy of the constructed ARG signature was stable and adequate in the GSE66229 cohort (the AUC of predicting 1-, 3- and 5-year OS was 0.59, 0.63 and 0.64, respectively; the AUC of predicting 1-, 3- and 5-year DFS was 0.57, 0.64 and 0.65, respectively, **Figure 6R, 6S**).

### *Identification of the molecular characteristics, and the efficacy of immunotherapy and targeted therapy*

As demonstrated in **Figure 7**, the percentage of patients with recurrent GC in the GSE26901

cohort was significantly different, and patients that suffered with disease recurrence exhibited significantly higher risk scores (**Figure 7A**). Moreover, the EMT subtype of GC was significantly higher than the other three GC subtypes, including MSI, TP53 positive and TP53 negative in GSE66229 (**Figure 7B**). The higher predicted capacity was concentrated in the GS subtype, compared with the CIN, POLE, MSI and EBV infection subtypes (**Figure 7C**). The low-risk score group presented an increased tumor mutational burden compared with the high score group (**Figure 7D, 7E**), and the Kaplan-Meier curves demonstrated that patients with the low-risk score exhibited an improved prognosis compared with those with the high-score in the IMvigor210 dataset (**Figure 7F**). Patients who responded to anti-PD-1/L1 immunotherapy exhibited lower low-risk scores compared with those without response ( $P=0.051$ , **Figure 7G**). In addition, the mutation counts, FGFR4 and HER2 were significantly negatively correlated with the risk score (**Figure 7H**). Notably, in accordance with angiogenesis, patients with a high ARG subtype score exhibited a significantly lower  $IC_{50}$  level of specific VEGF and PDGF receptor inhibitors, which may inhibit angiogenesis and the development of tumors. These included suni-

# Angiogenesis related genes-associated signature of gastric cancer

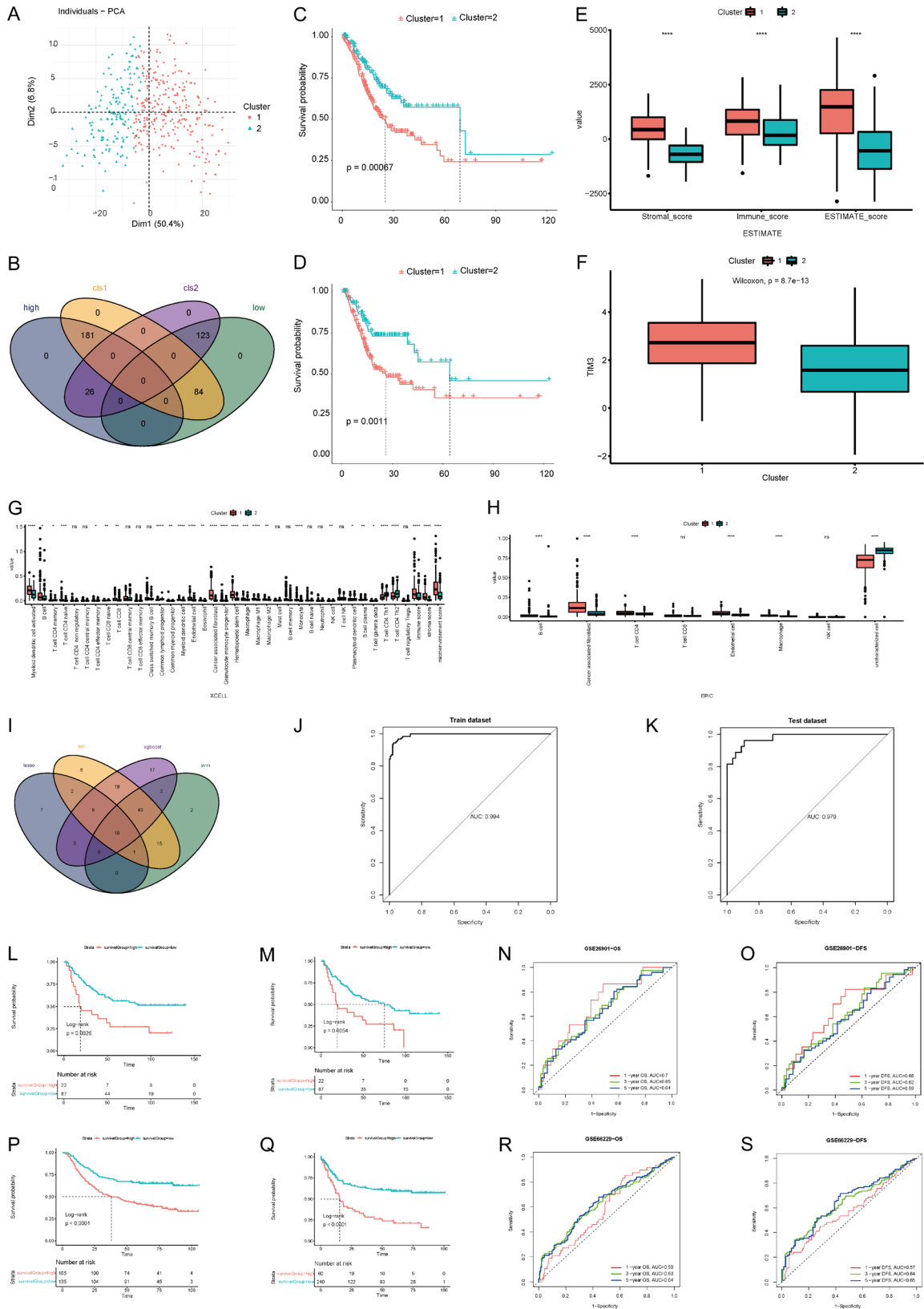


**Figure 6.** Construction and validation of an ARGs subtype predictor. (A) Principal component analysis (PCA) of the two clusters (cluster 1 and 2) in the TCGA cohort. (B) A Venn diagram of different expression genes of different clusters. The Kaplan-Meier curves for the OS (C) and DFS (D) of patients in the TCGA cohort, which was divided into cluster 1 and cluster 2 group. (E) Comparison of the immune score, stromal score, and ESTIMATE score between cluster

## Angiogenesis related genes-associated signature of gastric cancer

1 and cluster 2. (F) The expression level of TIM3 in the two clusters. Comparison of the contents of infiltrating immune cells between cluster 1 and cluster 2 was conducted by ESTIMATE (G) and XCELL (H). (I) A 10 most critical subtype specific genes were identified by Venn diagram, which were shared by four feature selection algorithms. ROC curves of the subtype predictor in distinguishing two subtypes in the train set (J) and test set (K). Kaplan-Meier survival analysis also suggested that patients' OS and PFS were significantly different between Subtype I and II both in GSE26901 (L and M) cohort. ROC curves showing the 1-, 3-, and 5-year OS (N) and DFS (O) predictive efficiency of the ARGs-signature in the GSE26901 cohort. Kaplan-Meier survival analysis also suggested that OS and PFS of patients were markedly different between Subtype I and II both in GSE66229 cohort (P, Q). (J, K) ROC curves showing the 1-, 3-, and 5-year OS (R) and DFS (S) predictive efficiency of the ARGs-signature in the GSE66229 cohort. ROC: Receiver operating characteristic; OS: overall survival; DFS: disease-free survival.

tinib, sorafenib, pazopanib and axitinib. Although these drugs have not been approved for GC treatment to date, patients with GC with a high-risk signature score may experience promising benefits from anti-angiogenesis therapy (Figure 7I).

### Discussion

In the present study, we developed a risk stratification system that predicts GC patients' survival from ARG feature, and verified its accuracy on independent validation datasets. The ARG score and related risk model could robustly and stably predict patient outcomes, having correlation with TME and immune feature. Furthermore, we also found the application value of the established risk score in treatment efficacy.

Angiogenesis plays a crucial role in tissue repair and regeneration in physiological and pathological processes, and is one of the hallmark events in cancer development [18]. Under normal physiological conditions, endothelial cells are sensitive to angiogenic signals and involved in angiogenesis by maintaining a high degree of plasticity. In contrast, in many disease states, including cancer, rheumatoid arthritis and atherosclerosis, aberrant angiogenesis will further accelerate the progression of these diseases, and is considered a hallmark of these disease states [19]. Previous evidence revealed that identified ARG may be used as a prognostic marker for the survival of patients with GC [20]. Results of the present study demonstrated that the survivals of patients with GC were significantly decreased in the high-ARG score group compared with those in the low-ARG score group, which is in consistent with previous research [21]. These results further supported that the ARG signature may act as an important prognostic prediction marker for GC patients.

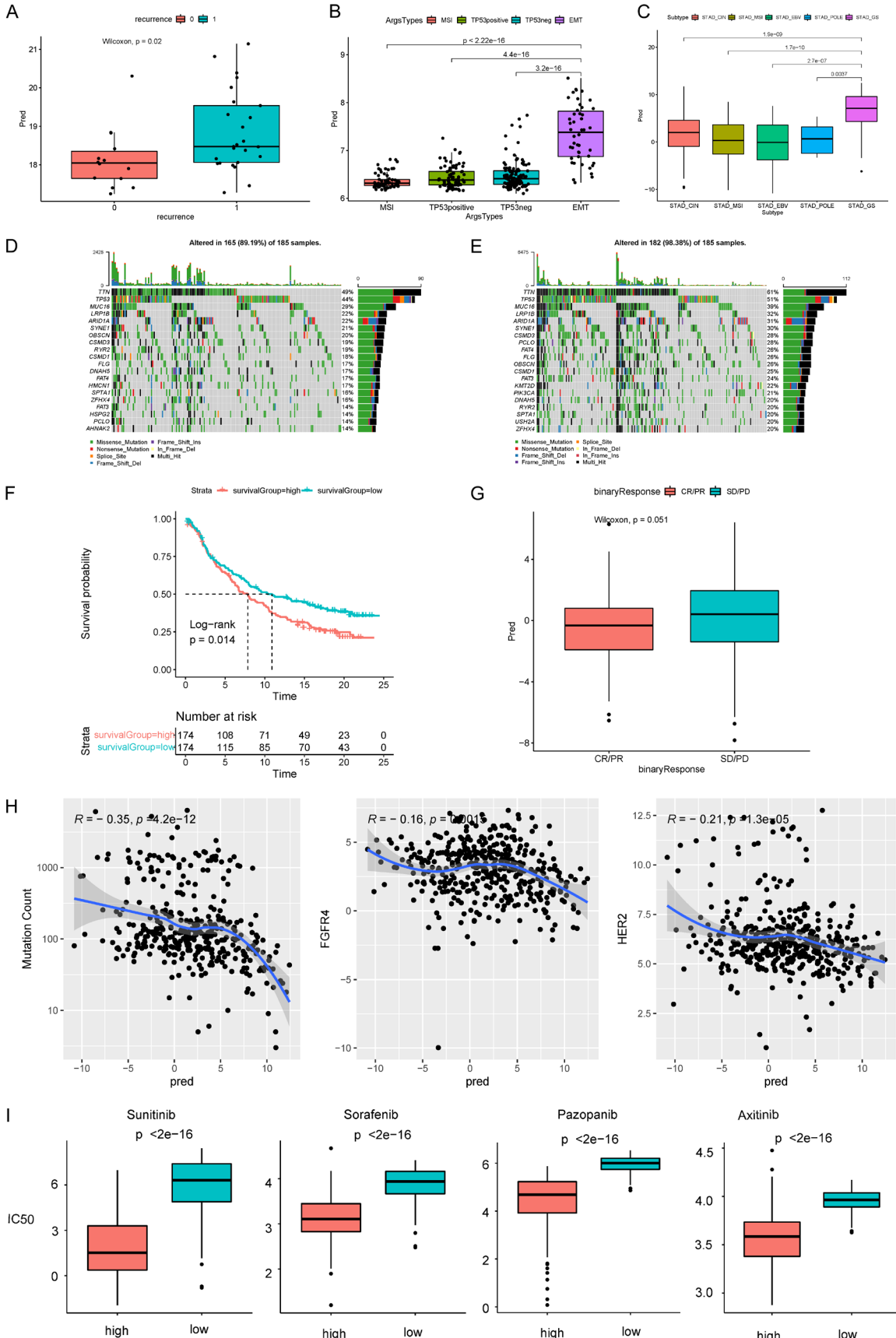
Angiogenesis interacts with TME in cancer, and cell contents in TME interact with surrounding cells via the circulatory and lymphatic systems

to further impact the development and progression of cancer [22]. The TME is mainly composed of three types of cell components, endothelial cells, immune cells (granulocytes, lymphocytes and macrophages) and fibroblasts [23]. GC patients with high ARGs score had significantly higher abundance of CAFs, which are a major component of the tumor stroma and crucial in facilitating crosstalk between cancer cells and the TME. Previous studies have demonstrated that CAF and endothelial cells play important roles in tumor cell proliferation, tumor angiogenesis, escaping from immune surveillance and metastasis [24]. Meanwhile, CAFs could promote breast cancer cell invasion by inducing the upregulation of genes involved in angiogenesis [25]. In addition, results of numerous previous studies revealed that CAFs increased angiogenesis by inducing the aberrant expression of key angiogenic factors. We also found that GC patients with both high abundance of mCAF and high ARG score had the most inferior survival.

We identified 10 key genes related to the ARG subtype, and the majority of them have been suggested as oncogenes that promote tumor development, invasion and metastasis in GC, including DCLK1 [26], NUDT10 [27], PTGIS [28], CHRDL1 [29] AGTR1 [30] and CNTN1 [31]. Previous studies suggested that most of these oncogenes could promote tumor by regulation TME, inducing EMT and angiogenesis in tumor [32]. In contrast, PCDH9 [33] and ECRG4 [34] were regarded as tumor suppressers in GC. Further in vitro and or in vivo studies are merited to give deep insights on how these genes regulating angiogenesis and tumor development in GC, and whether they could be therapeutically targeted to improve patients' survival.

To date, chemotherapy remains the cornerstone of the systemic treatment for patients with unresectable advanced or recurrent GC,

# Angiogenesis related genes-associated signature of gastric cancer



## Angiogenesis related genes-associated signature of gastric cancer

**Figure 7.** Identification of molecular characteristics related to risk score, and association analysis between the ARGs score and immunotherapy or targeted therapy. (A) The comparison of recurrence percentage of the GC patients. (B) The comparison of the four different ARGs types including MSI, TP53 positive, TP53 negative and EMT in GSE66229. (C) Differences in risk score among different TCGA-STAD molecular subtypes. The upper and lower ends of the boxes represented interquartile range of values. The lines in the boxes represented median value. The Kruskal-Wallis test was used to compare the statistical difference in risk score among five molecular subtypes. (D and E) The waterfall plot of tumor genetic mutation established by those with high risk score (D) and low risk score (E). Each column indicates individual patients. The upper bar plot showed TMB, and the number on the right indicated the mutation frequency in each gene. The right bar plot showed the proportion of each variant type. (F) Kaplan-Meier curves of overall survival according to ARGs score subtypes in the IMvigor210 cohort. (G) Boxplot illustrating the distribution of ARGs score for patients with different anti-PD-L1 immunotherapy responses in the IMvigor210 cohort. Significance was determined by the Wilcoxon test. SD, stable disease; PD, progressive disease; CR, complete response; PR, partial response. (H) The correlation between mutation counts, FGFR4, HER2 and ARGs score. (I) The difference in the  $IC_{50}$  of sunitinib, sorafenib, pazopanib and axitinib between samples with high- or low-risk score. TMB: tumor mutation burden;  $IC_{50}$ : half-maximal inhibitory concentration.

but with only limited benefits in improving both the PFS and OS [34]. The development of precision medicine, including targeted and immune therapies, are of urgent needs to overcome the treatment dilemma of GC. Notably, the finally established ARG subtype predictor risk score could not only robustly and stably predict patients' prognosis but also provide indications for therapeutic efficacy. Anti-angiogenesis therapy, especially those targeted at VEGF and its receptor, has shown promising antitumor efficacy in multiple types of cancers, including gastric cancer. Antibody blockade-based (bevacizumab [35] and ramucirumab [36] and tyrosine kinase inhibitor (TKI)-based strategies (lotinib and apatinib [37]) have been approved to use as monotherapy or combination with chemotherapy for gastric cancer by the USA and Chinese administrations. Some other TKIs, including sorafenib, sunitinib, pazopanib and axitinib have shown clinical benefits by combining with chemotherapy in patients with GC [38]. In this study, we found albeit high-risk patients had worse survival, and they were more sensitive to these anti-angiogenesis TKIs, which is in consistent with the mechanism how the predictor constructed. Another emerging novel therapy for GC is the immune checkpoint inhibitors. However, they were only efficacious to small part of patients. MSI and TMB are the FDA-approved pan-cancer biomarkers associated with better clinical outcomes treated with pembrolizumab, an anti-PD-1 blockade, and have been proved in the GC [39]. Interestingly, we found that the risk score was significantly negatively correlated with the TMB, and patients in the MSI subtype had the lowest risk score. In concordance with these results, high risk patients had inferior survivals and lower response rate to atezolizumab based on analysis

of the IMvigor210. Furthermore, we found the risk score was also negatively correlated with ERBB2 and FGFR4 levels. ERBB2, also known as HER2, is overexpressed in 10-30% of GC and is one of the most important actionable biomarkers in GC. Multiple targeted strategies, including antibodies, antibody drug conjugate (ADC) and TKIs had proved promising anti-tumor effects in GC [40]. In addition, recent clinical trials, such as KEYNOTE-811, further provided clinical rationales for the combination of anti-HER2 and anti-PD-1/L1 for treating HER2-positive GC patients [41]. In short, these results provided potential treatment stratification for GC patients, and patients with higher risk score may have better clinical benefits from anti-angiogenesis therapy but lower possibility to response to anti-HER2 and/or immune checkpoint blockades.

In conclusion, this study confirmed the prognostic role of ARGs and its correlation between ARGs and TME, especially CAFs in GC. In addition, a 10-gene based risk model was constructed, providing not only prognosis but also potential treatments stratification. However, this study has several limitations. First, though the performance of the established ARG and related prognostic signature was stable and robust, the construction and validation of them were all based on the public data. So, a confirmatory test using local tumor tissue samples from patients with gastric cancer needs to be carried out in future. Second, the mechanisms of the identified 10 genes involved in ARG subtype predictor in regulating tumor angiogenesis and development are still unknown. Further in vitro or in vivo study is merited to clarify the biology function.

## Acknowledgements

This work was supported in part by a grant from the National Natural Science Foundation of China (NSFC No. 82002122) and Changning district medical and health research projects of Shanghai (CNKW2018Y35) to Ning Ma, National Natural Science Foundation of China (NSFC No. 81472479) to Bin Wang and Foundation of Naval Medical University (2021QN26) to Jie Li.

## Disclosure of conflict of interest

None.

**Address correspondence to:** Bin Wang, Department of Oncology, Changhai Hospital, Naval Medical University, 168 Changhai Road, Shanghai 200433, P. R. China. Tel: +86-13764528043; E-mail: qcwangb@163.com; Kainan Li, Department of Oncology, Shandong Provincial Third Hospital, Cheeloo College of Medicine, Shandong University, 11 Wuyingshan Middle Road, Jinan 250031, Shandong, P. R. China. Tel: +86-15053125301; E-mail: henrylee145@126.com; Chunhua Li, Department of Oncology, The Second Affiliated Hospital of Shandong University of Traditional Chinese Medicine, Jingba Road #1, Jinan 250001, Shandong, P. R. China. Tel: +86-15553119168; E-mail: lichunhua82436539@163.com

## References

- [1] Smyth EC, Nilsson M, Grabsch HI, van Grieken NC and Lordick F. Gastric cancer. *Lancet* 2020; 396: 635-648.
- [2] Serra O, Galán M, Ginesta MM, Calvo M, Sala N and Salazar R. Comparison and applicability of molecular classifications for gastric cancer. *Cancer Treat Rev* 2019; 77: 29-34.
- [3] Cheong JH, Wang SC, Park S, Porembka MR, Christie AL, Kim H, Kim HS, Zhu H, Hyung WJ, Noh SH, Hu B, Hong C, Karalis JD, Kim IH, Lee SH and Hwang TH. Development and validation of a prognostic and predictive 32-gene signature for gastric cancer. *Nat Commun* 2022; 13: 774.
- [4] Wang J, Kunzke T, Prade VM, Shen J, Buck A, Feuchtinger A, Haffner I, Luber B, Liu DHW, Langer R, Lordick F, Sun N and Walch A. Spatial metabolomics identifies distinct tumor-specific subtypes in gastric cancer patients. *Clin Cancer Res* 2022; 21: 4383.
- [5] Carmeliet P. Angiogenesis in life, disease and medicine. *Nature* 2005; 438: 932-936.
- [6] Oshi M, Newman S, Tokumaru Y, Yan L, Matsuyama R, Endo I, Nagahashi M and Takabe K. Intra-tumoral angiogenesis is associated with inflammation, immune reaction and metastatic recurrence in breast cancer. *Int J Mol Sci* 2020; 21: 6708.
- [7] Wan XY, Guan SD, Hou YX, Qin YL, Zeng H, Yang LP, Qiao YN, Liu SQ, Li Q, Jin T, Qiu YX and Liu MR. FOSL2 promotes VEGF-independent angiogenesis by transcriptionally activating Wnt5a in breast cancer-associated fibroblasts. *Theranostics* 2021; 11: 4975-4991.
- [8] Roviello G, Petrioli R, Marano L, Polom K, Marrelli D, Perrella A and Roviello F. Angiogenesis inhibitors in gastric and gastroesophageal junction cancer. *Gastric Cancer* 2016; 19: 31-41.
- [9] Feng Y, Dai Y, Gong ZH, Cheng JN, Zhang LH, Sun CD, Zeng XH, Jia QZ and Zhu B. Association between angiogenesis and cytotoxic signatures in the tumor microenvironment of gastric cancer. *Onco Targets Ther* 2018; 11: 2725-2733.
- [10] Min KW, Kim DH, Noh YK, Son BK, Kwon MJ and Moon JY. Cancer-associated fibroblasts are associated with poor prognosis in solid type of lung adenocarcinoma in a machine learning analysis. *Sci Rep* 2021; 11: 16779.
- [11] Dayan D, Salo T, Salo S, Nyberg P, Nurmenniemi S, Costea DE and Vered M. Molecular cross-talk between cancer cells and tumor microenvironment components suggests potential targets for new therapeutic approaches in mobile tongue cancer. *Cancer Med* 2012; 1: 128-140.
- [12] Hanley CJ, Mellone M, Ford K, Thirdborough SM, Mellows T, Frampton SJ, Smith DM, Harden E, Szyndralewicz C, Bullock M, Noble F, Moutasim KA, King EV, Vijayanand P, Mirnezami AH, Underwood TJ, Ottensmeier CH and Thomas GJ. Targeting the myofibroblastic cancer-associated fibroblast phenotype through inhibition of NOX4. *J Natl Cancer Inst* 2018; 110: 109-120.
- [13] Liu L, Liu L, Yao HH, Zhu ZQ, Ning ZL and Huang Q. Stromal myofibroblasts are associated with poor prognosis in solid cancers: a meta-analysis of published studies. *PLoS One* 2016; 11: e0159947.
- [14] Li J, Liu X, Zang SZ, Zhou JS, Zhang FY, Sun B, Qi DY, Li XJ, Kong J, Jin D, Yang XS, Luo Y, Lu Y, Lin BC, Niu WD and Liu TJ. Small extracellular vesicle-bound vascular endothelial growth factor secreted by carcinoma-associated fibroblasts promotes angiogenesis in a bevacizumab-resistant manner. *Cancer Lett* 2020; 492: 71-83.
- [15] Sauerbrei W, Royston P and Binder H. Selection of important variables and determination

## Angiogenesis related genes-associated signature of gastric cancer

- of functional form for continuous predictors in multivariable model building. *Stat Med* 2007; 26: 5512-5528.
- [16] Yperman J, Becker T, Valkenburg D, Popescu V, Hellings N, Wijmeersch BV and Peeters LM. Machine learning analysis of motor evoked potential time series to predict disability progression in multiple sclerosis. *BMC Neurol* 2020; 20: 105.
- [17] Li W, Yin YB, Quan XW and Zhang H. Gene expression value prediction based on XGBoost algorithm. *Front Genet* 2019; 10: 1077.
- [18] Zheng WZ, Zhang SQ, Guo H, Chen XB, Huang ZC, Jiang SQ and Li MQ. Multi-omics analysis of tumor angiogenesis characteristics and potential epigenetic regulation mechanisms in renal clear cell carcinoma. *Cell Commun Signal* 2021; 19: 39.
- [19] Carmeliet P and Jain RK. Molecular mechanisms and clinical applications of angiogenesis. *Nature* 2011; 473: 298-307.
- [20] He LN, Feng AQ, Guo H, Huang HH, Deng QC, Zhao ED and Yang M. LRG1 mediated by ATF3 promotes growth and angiogenesis of gastric cancer by regulating the SRC/STAT3/VEGFA pathway. *Gastric Cancer* 2022; 25: 527-541.
- [21] Zheng S, Zhang ZZ, Ding N, Sun JW, Lin YF, Chen JY, Zhong J, Shao LM, Lin ZH and Xue M. Identification of the angiogenesis related genes for predicting prognosis of patients with gastric cancer. *BMC Gastroenterol* 2021; 21: 146.
- [22] Nicole MA and Simon MC. The tumor microenvironment. *Curr Biol* 2020; 30: R921-R925.
- [23] Hanahan D and Weinberg RA. Hallmarks of cancer: the next generation. *Cell* 2011; 144: 646-674.
- [24] Kalluri R and Zeisberg M. Fibroblasts in cancer. *Nat Rev Cancer* 2006; 6: 392-401.
- [25] Eiro N, González L, Martínez-Ordoñez A, Fernandez-Garcia B, González LO, Cid S, Dominguez F, Perez-Fernandez R and Vizoso FJ. Cancer-associated fibroblasts affect breast cancer cell gene expression, invasion and angiogenesis. *Cell Oncol (Dordr)* 2018; 41: 369-378.
- [26] Wu XY, Qu DF, Weygant N, Peng J and Houchen CW. Cancer stem cell marker DCLK1 correlates with tumorigenic immune infiltrates in the colon and gastric adenocarcinoma microenvironments. *Cancers (Basel)* 2020; 12: 274.
- [27] Chen DQ, Zhang RX, Xie AS, Yuan JP, Zhang JH, Huang YJ, Zhang HX and Zhang FR. Clinical correlations and prognostic value of Nudix hydroxylase 10 in patients with gastric cancer. *Bioengineered* 2021; 12: 9779-9789.
- [28] Dai DN, Chen B, Feng YL, Wang WZ, Jiang YH, Huang H and Liu JH. Prognostic value of prostaglandin I2 synthase and its correlation with tumor-infiltrating immune cells in lung cancer, ovarian cancer, and gastric cancer. *Aging (Albany NY)* 2020; 12: 9658-9685.
- [29] Wang J, Ding YR, Wu YY and Wang XX. Identification of the complex regulatory relationships related to gastric cancer from lncRNA-miRNA-mRNA network. *J Cell Biochem* 2020; 121: 876-887.
- [30] Xu X, Lu YD, Wu YL, Wang ML, Wang XD, Wang HZ, Chen B and Li YX. A signature of seven immune-related genes predicts overall survival in male gastric cancer patients. *Cancer Cell Int* 2021; 21: 117.
- [31] Chen DH, Yu JW and Jiang BJ. Contactin 1: a potential therapeutic target and biomarker in gastric cancer. *World J Gastroenterol* 2015; 21: 9707-9716.
- [32] Chen Y, Xiang HG, Zhang YF, Wang JJ and Yu GZ. Loss of PCDH9 is associated with the differentiation of tumor cells and metastasis and predicts poor survival in gastric cancer. *Clin Exp Metastasis* 2015; 32: 417-428.
- [33] You YJ and Hu SJ. Dysregulation of ECRG4 is associated with malignant properties and of prognostic importance in human gastric cancer. *Cancer Biomark* 2022; 34: 55-66.
- [34] Muro K, Van Cutsem E, Narita Y, Pentheroudakis G, Baba E, Li J, Ryu MH, Zamanih WIW, Yong WP, Yeh KH, Kato K, Lu Z, Cho BC, Nor IM, Ng M, Chen LT, Nakajima TE, Shitara K, Kawakami H, Tsushima T, Yoshino T, Lordick F, Martinelli E, Smyth EC, Arnold D, Minami H, Taberero J and Douillard JY. Pan-Asian adapted ESMO clinical practice guidelines for the management of patients with metastatic gastric cancer: a JSMO-ESMO initiative endorsed by CSCO, KSMO, MOS, SSO and TOS. *Ann Oncol* 2019; 30: 19-33.
- [35] Ohtsu A, Shah MA, Van Cutsem E, Rha SY, Sawaki A, Park SR, Lim HY, Yamada Y, Wu J, Langer B, Starnawski M and Kang YK. Bevacizumab in combination with chemotherapy as first-line therapy in advanced gastric cancer: a randomized, double-blind, placebo-controlled phase III study. *J Clin Oncol* 2011; 29: 3968-3976.
- [36] Wilke H, Muro K, Van Cutsem E, Oh SC, Bodoky G, Shimada Y, Hironaka S, Sugimoto N, Lipatov O, Kim TY, Cunningham D, Rougier P, Komatsu Y, Ajani J, Emig M, Carlesi R, Ferry D, Chandrawansa K, Schwartz JD and Ohtsu A; RAINBOW Study Group. Ramucirumab plus paclitaxel versus placebo plus paclitaxel in patients with previously treated advanced gastric or gastro-oesophageal junction adenocarcinoma (RAINBOW): a double-blind, randomised phase 3 trial. *Lancet Oncol* 2014; 15: 1224-1235.
- [37] Xia L, Zhou F, Dai J, Jiang H, Yang L, Wang W, Peng J and Gong J. Apatinib in combination with docetaxol and S1 chemotherapy in the

## Angiogenesis related genes-associated signature of gastric cancer

- first-line treatment of metastatic gastric cancer. *Ann Oncol* 2019.
- [38] Högner A, Al-Batran SE, Siveke JT, Lorenz M, Bartels P, Breithaupt K, Malfertheiner P, Homann N, Stein A, Gläser D, Tamm I, Hinke A, Vogel A and Thuss-Patience P; PaFLO investigators. Pazopanib with 5-FU and oxaliplatin as first line therapy in advanced gastric cancer: a randomized phase-II study-The PaFLO trial. A study of the Arbeitsgemeinschaft Internistische Onkologie AIO-STO-0510. *Int J Cancer* 2022; 150: 1007-1017.
- [39] Wang F, Wei XL, Wang FH, Xu N, Shen L, Dai GH, Yuan XL, Chen Y, Yang SJ, Shi JH, Hu XC, Lin XY, Zhang QY, Feng JF, Ba Y, Liu YP, Li W, Shu YQ, Jiang Y, Li Q, Wang JW, Wu H, Feng H, Yao S and Xu RH. Safety, efficacy and tumor mutational burden as a biomarker of overall survival benefit in chemo-refractory gastric cancer treated with toripalimab, a PD-1 antibody in phase Ib/II clinical trial NCT02915432. *Ann Oncol* 2019; 30: 1479-1486.
- [40] Taberero J, Hoff PM, Shen L, Ohtsu A, Shah MA, Cheng KR, Song CY, Wu HY, Eng-Wong J, Kim K and Kang YK. Pertuzumab plus trastuzumab and chemotherapy for HER2-positive metastatic gastric or gastro-oesophageal junction cancer (JACOB): final analysis of a double-blind, randomised, placebo-controlled phase 3 study. *Lancet Oncol* 2018; 19: 1372-1384.
- [41] Janjigian YY, Kawazoe A, Yañez P, Li N, Lonardi S, Kolesnik O, Barajas O, Bai Y, Shen L, Tang Y, Wyrwicz LS, Xu J, Shitara K, Qin S, Van Cutsem E, Taberero J, Li L, Shah S, Bhagia P and Chung HC. The KEYNOTE-811 trial of dual PD-1 and HER2 blockade in HER2-positive gastric cancer. *Nature* 2021; 600: 727-730.

# Angiogenesis related genes-associated signature of gastric cancer

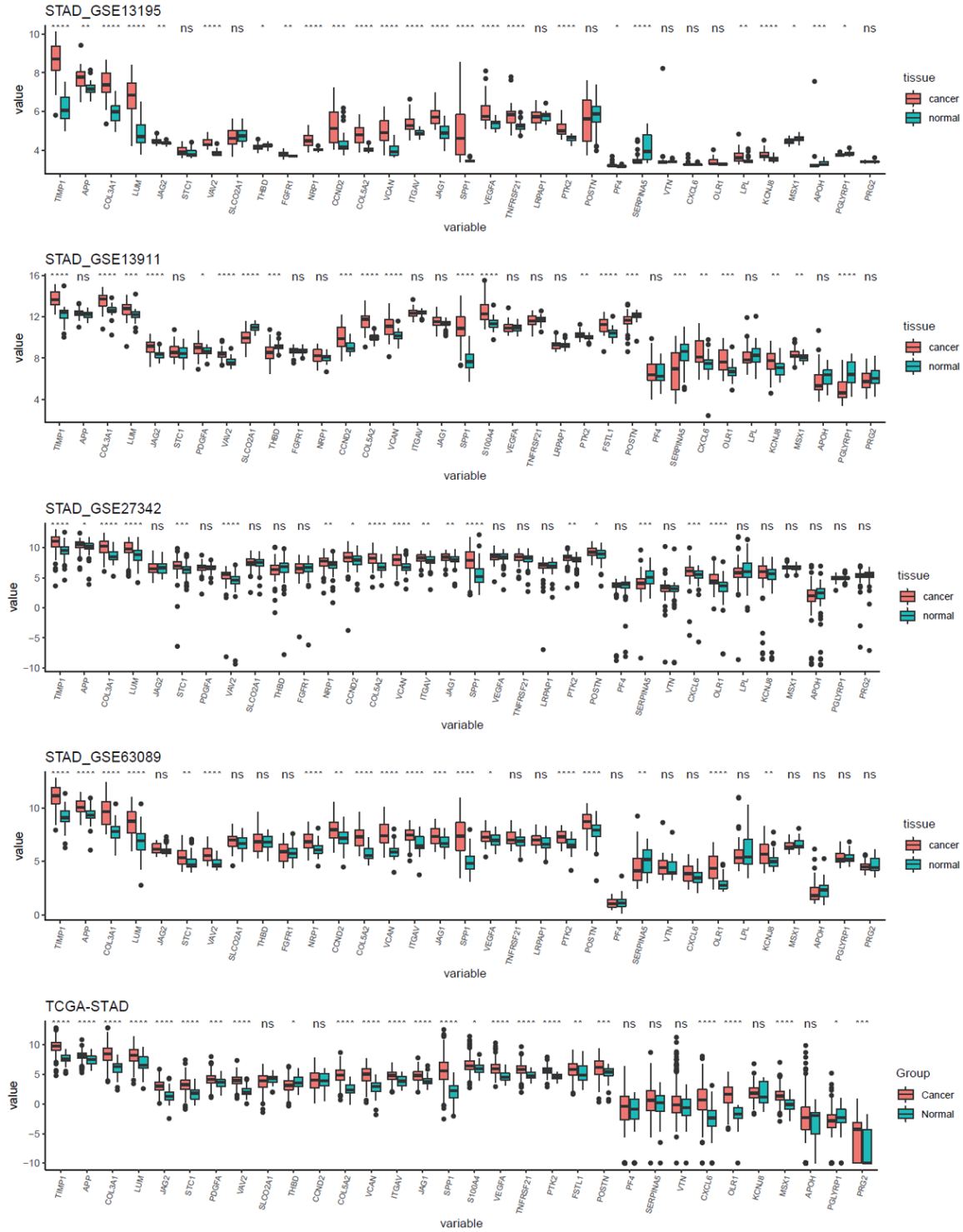


**Figure S1.** Comparison of the expression level 36 ARGs between normal and tumor samples in TCGA-GC, GSE13195, GSE13911, GSE27342 and GSE63089 datasets. \*P<0.05; \*\*P<0.01; \*\*\*P<0.001; \*\*\*\*P<0.0001; ns: not significant.

## Angiogenesis related genes-associated signature of gastric cancer

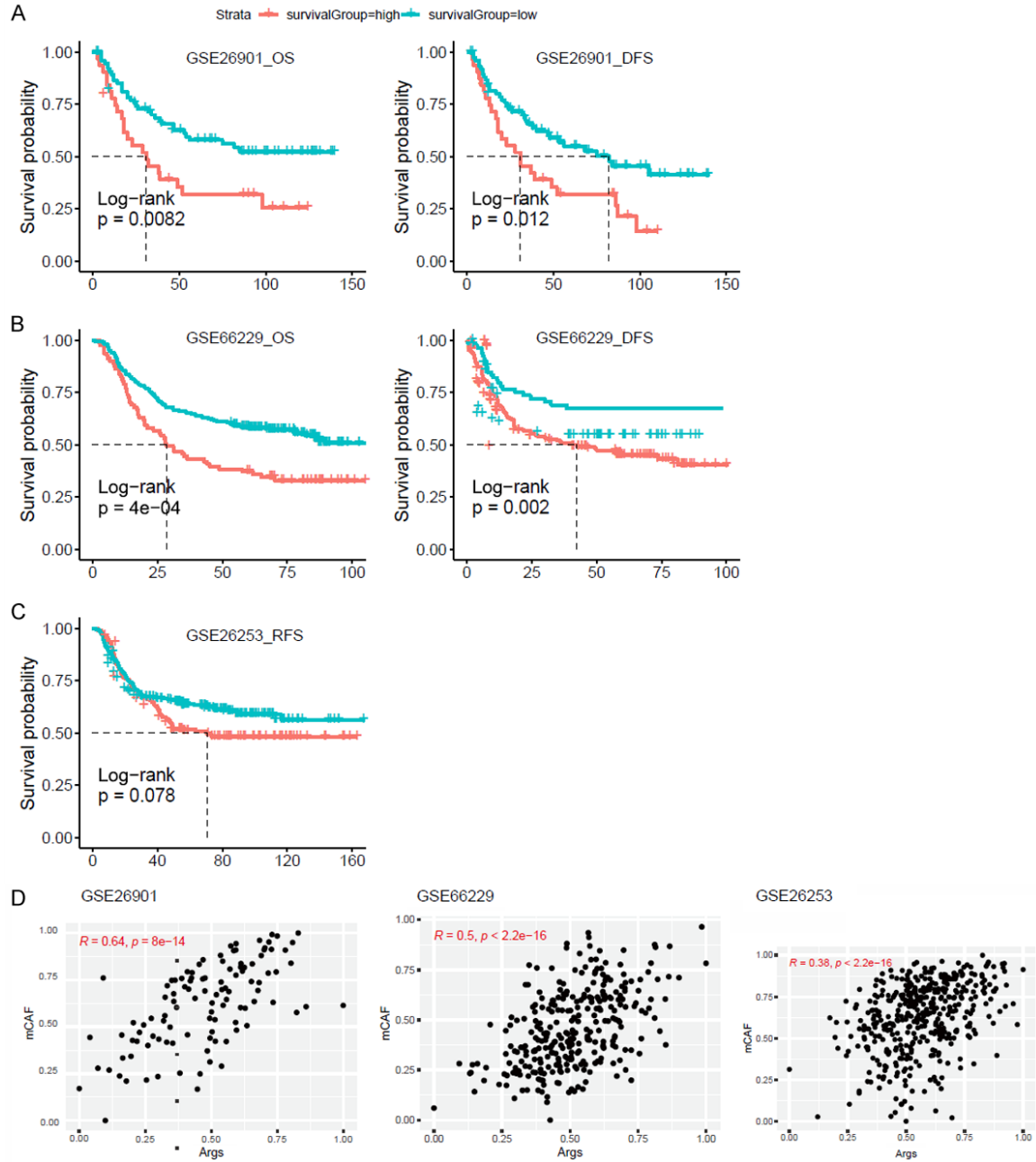


**Figure S2.** Association between CAFs subtypes and ARG signature in GC patients in three validation cohorts. The difference in the survival between high- and low-ARG risk score in GSE26901 (A), GSE66229 (B) and GSE26253 (C). (D) The correlation between ARGs and matrix cancer-associated fibroblasts (mCAFs). OS: overall survival; DFS: disease-free survival; RFS: recurrence.



# Angiogenesis related genes-associated signature of gastric cancer

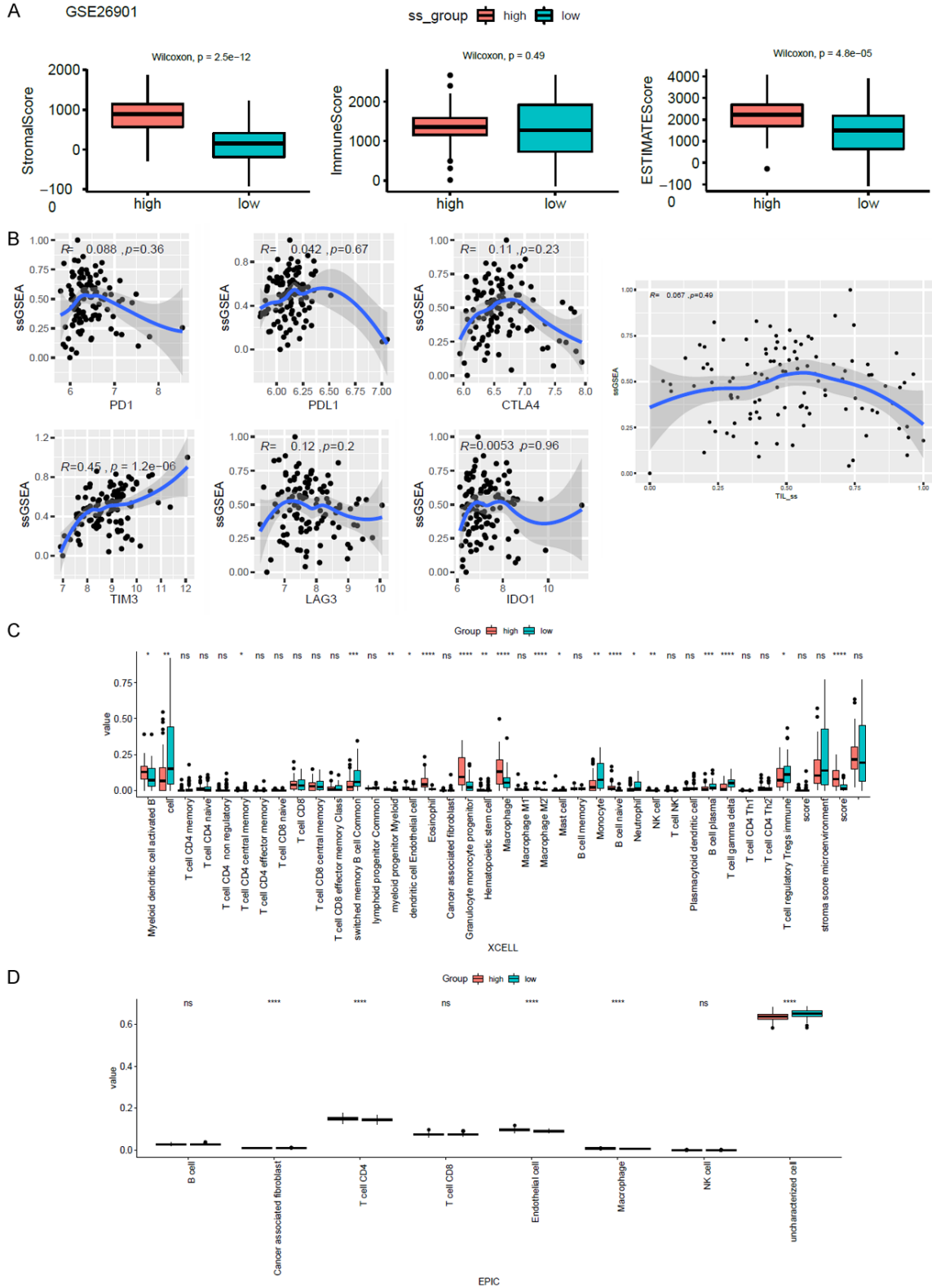


**Figure S4.** ARGs signature associated tumor microenvironment analysis in GSE26901. (A) The difference in Stromal, Immune and ESTIMATE score between high- and low-ARGs score samples in GSE26901. (B) Correlations between ARG score and TILs, ICGs (CTLA4, TIM3, LAG3 and IDO1) were analyzed by Spearman analysis. Tumor-infiltrated immune cells were analyzed by XCELL (C) and EPIC (D). \* $P < 0.05$ ; \*\* $P < 0.01$ ; \*\*\* $P < 0.001$ ; \*\*\*\* $P < 0.0001$ ; ns: not significant.

# Angiogenesis related genes-associated signature of gastric cancer

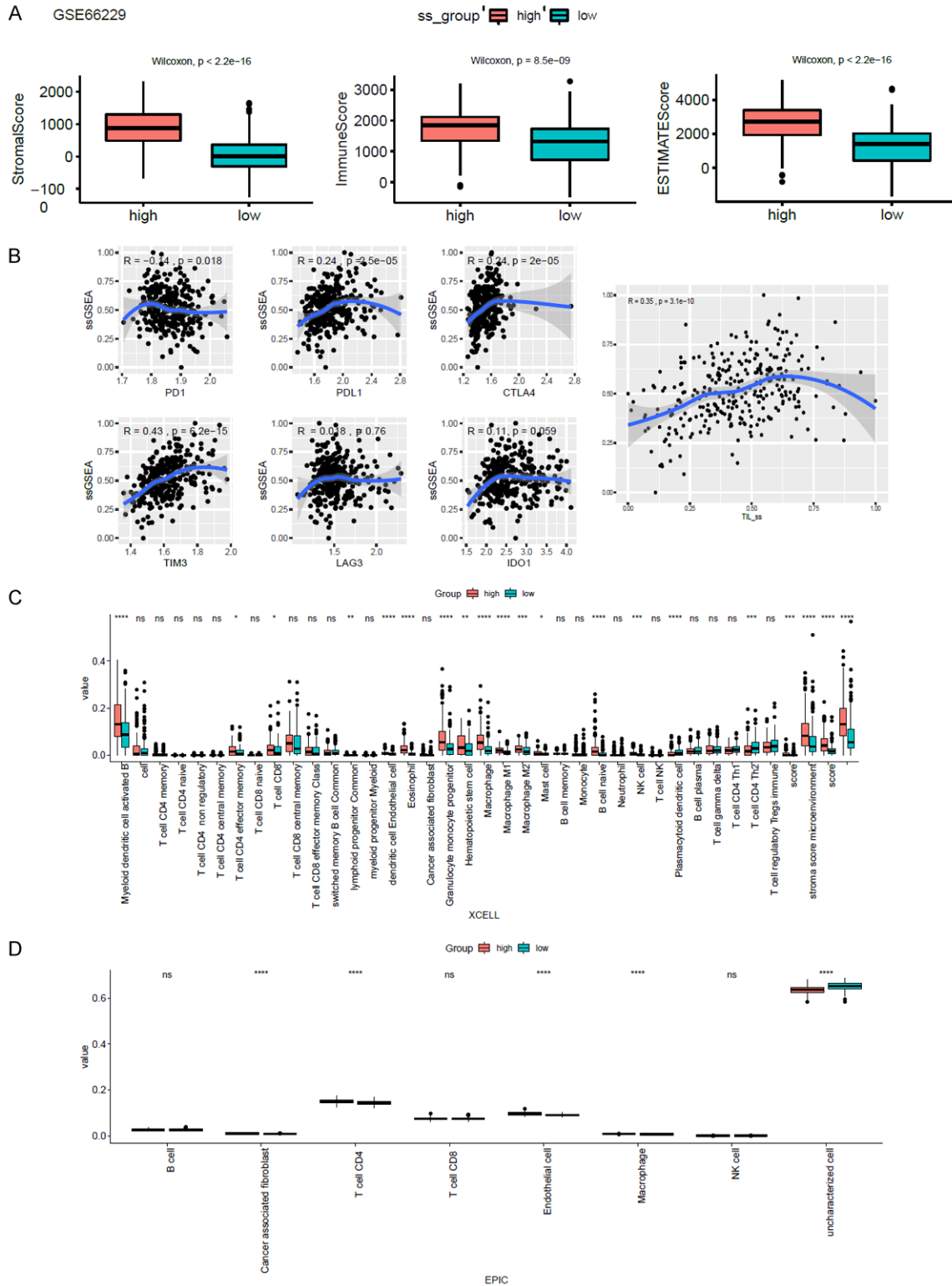


**Figure S5.** ARGs signature associated tumor microenvironment analysis in GSE66229. (A) The difference in Stromal, Immune and ESTIMATE score between high- and low-ARGs score samples in GSE66229. (B) Correlations between ARG score and TILs, ICGs (CTLA4, TIM3, LAG3 and IDO1) were analyzed by Spearman analysis. Tumor-infiltrated immune cells were analyzed by XCELL (C) and EPIC (D). \* $P < 0.05$ ; \*\* $P < 0.01$ ; \*\*\* $P < 0.001$ ; \*\*\*\* $P < 0.0001$ ; ns: not significant.